AGU PUBLICATIONS

JGR

Journal of Geophysical Research: Space Physics

RESEARCH ARTICLE

10.1002/2013JA019249

Key Points:

- A quadrupole structure forms inside an island during antiparallel reconnection
- With a guide field,the magnetic field is enhanced with a dip in the center
- Magnetic field is enhanced at one end of a magnetic island in asymmetric case

Correspondence to:
Q. Lu,
qmlu@ustc.edu.cn

Citation:
Huang, C., Q. Lu, S. Lu, P. Wang, and S. Wang (2014), The effect of a guide field on the structures of magnetic islands formed during multiple X line reconnections: Two-dimensional particle-in-cell simulations, *J. Geophys. Res. Space Physics*, *119*, 798–807, doi:10.1002/2013JA019249.

Received 24 JUL 2013
Accepted 30 DEC 2013
Accepted article online 6 JAN 2014
Published online 3 FEB 2014

The effect of a guide field on the structures of magnetic islands formed during multiple X line reconnections: Two-dimensional particle-in-cell simulations

Can Huang[1], Quanming Lu[1], San Lu[1], Peiran Wang[1], and Shui Wang[1]

[1]CAS Key Laboratory of Geospace Environment, Department of Geophysics and Planetary Science, University of Science and Technology of China, Hefei, China

Abstract A magnetic island plays an important role in magnetic reconnection. In this paper, using a series of two-dimensional particle-in-cell simulations, we investigate the magnetic structures of a magnetic island formed during multiple X line magnetic reconnections, considering the effects of the guide field in symmetric and asymmetric current sheets. In a symmetric current sheet, the current in the *x* direction forms a tripolar structure inside a magnetic island during antiparallel reconnection, which results in a quadrupole structure of the out-of-plane magnetic field. With the increase of the guide field, the symmetry of both the current system and out-of-plane magnetic field inside the magnetic island is distorted. When the guide field is sufficiently strong, the current forms a ring along the magnetic field lines inside a magnetic island. At the same time, the current carried by the energetic electrons accelerated in the vicinity of the X lines forms another ring at the edge of the magnetic island. Such a dual-ring current system enhances the out-of-plane magnetic field inside the magnetic island with a dip in the center of the magnetic island. In an asymmetric current sheet, when there is no guide field, electrons flow toward the X lines along the separatrices from the side with a higher density and are then directed away from the X lines along the separatrices to the side with a lower density. The formed current results in the enhancement of the out-of-plane magnetic field at one end of the magnetic island and the attenuation at the other end. With the increase of the guide field, the structures of both the current system and the out-of-plane magnetic field are distorted.

1. Introduction

Magnetic reconnection is a fundamental physical process which is used to explain the rapid conversion of magnetic energy into plasma kinetic and thermal energies [*Vasyliunas*, 1975; *Biskamp*, 2000; *Priest and Forbes*, 2000] in plasmas ranging from the solar atmosphere [*Giovanelli*, 1946; *Masuda et al.*, 1994] to the Earth's magnetosphere [*Baker et al.*, 1996; *Nagai et al.*, 1998; *Angelopoulos et al.*, 2008], and laboratory experiments [*Ji et al.*, 1998; *Li et al.*, 2007; *Dong et al.*, 2012].

The violation of the ideal condition, $\mathbf{E}+\mathbf{V}\times\mathbf{B}\neq 0$, is essential to allow the magnetic flux transport across the reconnection point, and the diffusion region, where the ideal condition is violated, is of strong interest for understanding magnetic reconnections. In collisionless magnetic reconnection, the ideal condition is different for ions and electrons due to their mass difference. The ions demagnetize on the scale of the ion inertial length, and the electrons demagnetize on the scale of the electron inertial length, which leads to the generation of the Hall magnetic field with a quadrupole structure in the diffusion region and the Hall electric field around separatrices [*Sonnerup*, 1979; *Terasawa*, 1983; *Birn et al.*, 2001; *Shay et al.*, 2001; *Øieroset et al.*, 2001; *Pritchett*, 2001; *Nagai et al.*, 2003; *Fu et al.*, 2006; *Lu et al.*, 2010a]. While a vast majority of reconnection studies consider symmetric cases with antiparallel magnetic field in the inflow region, some studies have shown that an added uniform magnetic field in the out-of-plane direction ("guide field") can introduce an asymmetry in the inflow direction, and the quadrupole structure of the out-of-plane magnetic field are distorted [*Pritchett and Coroniti*, 2004; *Huang et al.*, 2010; *Lu et al.*, 2011].

Magnetic island (also called magnetic flux rope when viewed in 3-D), formed between X lines, is also an important phenomena in magnetic reconnection. Electrons can be trapped in a magnetic island and get accelerated [*Drake et al.*, 2006a; *Chen et al.*, 2008; *Oka et al.*, 2010a, 2010b; *Wang et al.*, 2010], and these islands

Table 1. Summary of Simulations (Runs 1–5)[a]

Run	R	α_1	α_2	B_{y0}/B_0
1	0	0	1	0.0
2	0	0	1	0.1
3	0	0	1	1.0
4	1/2	1/3	1/3	0.0
5	1/2	1/3	1/3	1.0

[a]R denotes the asymmetry degree of the magnetic field, which is defined in equation (1).

may coalesce each other and the electrons can be accelerated with a higher efficiency [*Pritchett*, 2008; *Oka et al.*, 2010a, 2010b; *Tanaka et al.*, 2011; *Le et al.*, 2012]. Therefore, investigating the structures of magnetic islands is also essential for the understanding of magnetic reconnections. Simulations have shown that in antiparallel reconnection, a characteristic quadrupole pattern of the out-of-plane magnetic field is formed in a magnetic island [*Karimabadi et al.*, 1999, 2004; *Liu et al.*, 2009] , and such a structure has also been observed by satellite [*Deng et al.*, 2004; *Zhang et al.*, 2011]. In guide field magnetic reconnection, the out-of-plane magnetic field is enhanced in a magnetic island [*Ma et al.*, 1994; *Drake et al.*, 2006b; *Chen et al.*, 2008; *Daughton et al.*, 2011]. Recently, the out-of-plane magnetic field inside a magnetic island has been found to have more complicated structures by satellite observations. *Borg et al.* [2012] found that the amplitude of the out-of-plane magnetic field appears to have double peaks. *Lui et al.* [2007] suggest that while the outer layer of a flux rope has the expected helical shape, the inner layers may have a more irregular magnetic structure. With two-dimensional (2-D) particle-in-cell (PIC) simulations, *Huang et al.* [2012] found that in the magnetic island, which is formed during multiple X line magnetic reconnection, the in-plane current system exhibits a dual-ring structure. It results in a dip of the out-of-plane magnetic field in the center of the island, which is consistent with the double peak structure of the out-of-plane magnetic field observed by *Borg et al.* [2012]. In this paper, by performing a series of two-dimensional (2-D) particle-in-cell (PIC) simulations, we investigate the effect of a guide field on the structure of the magnetic island formed during multiple X line reconnection symmetric and asymmetric current sheets. The results show that the guide field has a significant influence on the structure of the magnetic island, and an explanation based on the current system formed inside the island is given.

The structure of the paper is as follows. In section 2, the simulation model is overviewed. The simulation results are presented in section 3. The conclusions and discussion are given in section 4.

2. Simulation Model

Two-dimensional PIC simulations are performed in this paper to investigate the structure of a magnetic island formed during multiple X line magnetic reconnections. The details of the PIC simulation model can be referred in *Birdsall and Langdon* [1985]. Periodic boundary conditions are assumed in the *x* direction, while in the *z* direction conducting boundary conditions are retained and particles are specularly reflected.

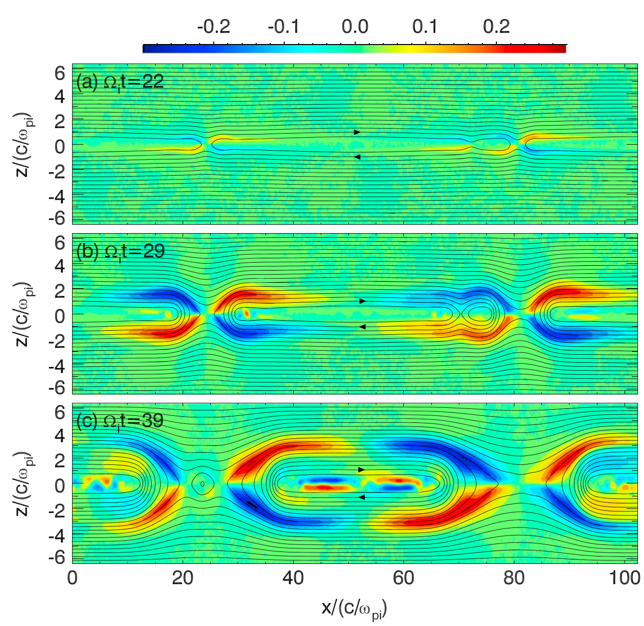

Figure 1. The time evolution of the out-of-plane magnetic field at (a) $\Omega_i t = 22$, (b) $\Omega_i t = 29$, and (c) $\Omega_i t = 39$ for Run 1. The in-plane magnetic field lines are also presented. The arrows denote the direction of the local magnetic field.

The initial equilibrium configuration of the asymmetric current in the (x, z) plane has been described by *Quest and Coroniti* [1981], and the profile of the magnetic field is given by the expression

$$\mathbf{B}_0(z) = B_0[\tanh(z/\delta) + R]\mathbf{e}_x + B_{y0}\mathbf{e}_y \quad (1)$$

where B_{y0} and δ are the amplitude of the guide field and the initial half width of the current sheet, respectively. The null point exists only if $|R| < 1$.

The temperatures of the ions and electrons are assumed to be homogeneous,

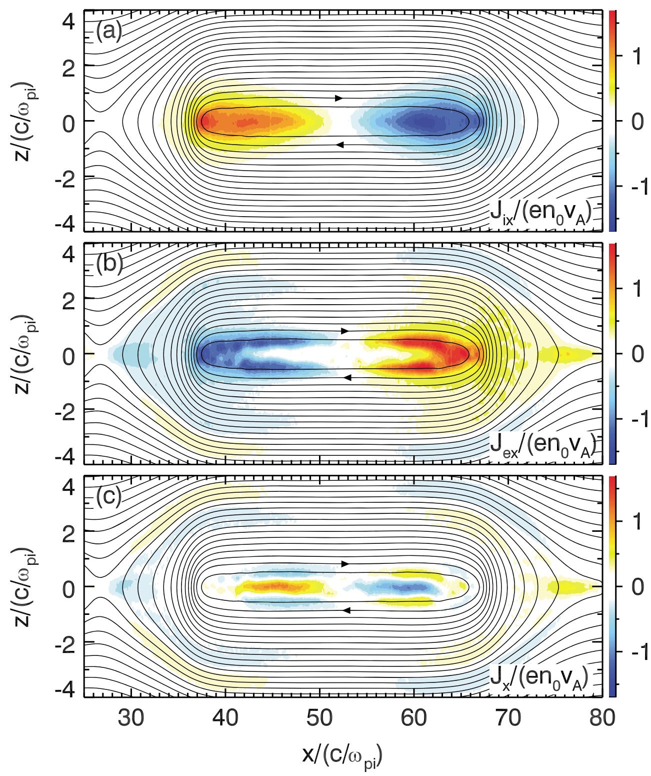

Figure 2. The (a) ion, (b) electron, and (c) total currents in the x direction at $\Omega_i t = 39$ for Run 1. The in-plane magnetic field lines are also presented. The arrows denote the direction of the local magnetic field.

and thus, the associated plasma density in the current sheet is given by

$$n(z) = n_0\left[1 - \alpha_1 \tanh(x/\delta) - \alpha_2 \tanh^2(x/\delta)\right], \qquad (2)$$

which implies a density drop by $2\alpha_1 n_0$ across the current sheet. In order to satisfy the pressure balance constraint, the parameters should be set to $\alpha_2 = B_0^2/2\mu_0 n_0(T_{i0}+T_{e0})$ and $\alpha_1 = 2R\alpha_2$. When $\alpha_1 = R = 0$ and $\alpha_2 = 1$, one recovers the usual symmetric Harris current sheet [*Harris*, 1962].

We choose $\delta = 0.5\ c/\omega_{pi}$ (where c/ω_{pi} is the ion inertial length based on the density n_0). The distributions of the ions and electrons are assumed to satisfy the Maxwellian function with drift speeds in the y direction. The drift speeds of the ions and electrons satisfy the equation $V_{i0}/V_{e0} = -T_{i0}/T_{e0}$ (where $V_{i0}(V_{e0})$ and $T_{i0}(T_{e0})$ are the initial drift speed and temperature of the ions (electrons), respectively). The initial temperature ratio of the ions to the electrons is set to be $T_{i0}/T_{e0} = 4$. The mass ratio of the ion to the electron is $m_i/m_e = 100$ and the light speed is $c = 15v_A$ (where v_A is the Alfven speed based on B_0 and n_0).

The simulations are performed in the (x,z) plane. The box dimensions are $L_x = 102.4\ c/\omega_{pi}$ in the x direction and $L_z = 25.6\ c/\omega_{pi}$ in the z direction with the spatial resolution $\Delta x = \Delta z = 0.05\ c/\omega_{pi} = 0.5\ c/\omega_{pe}$ (where c/ω_{pe} is the electron inertial length based on n_0). The time step is set to $\Omega_i \Delta t = 0.001$, where $\Omega_i = eB_0/m_i$ is the ion gyrofrequency. More than 10^8 particles per species are employed in the simulations. In all runs, reconnection is triggered by a small flux perturbation.

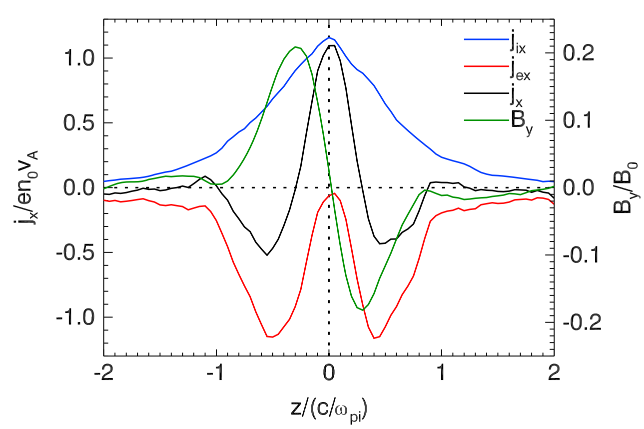

Figure 3. The profiles of the ion (blue), electron (red), total (black) current in the x direction, and out-of-plane magnetic field B_y (green) along the line $x = 45c/\omega_{pi}$ at $\Omega_i t = 39$ for Run 1.

3. Simulation Results

By changing the amplitude of the initial guide field, we investigate their effects on the structures of magnetic islands formed during multiple X line reconnections in symmetric and asymmetric current sheets, and a total of five cases are run. Runs 1–3 consider magnetic reconnection in a symmetric current, while in Runs 4 and 5 magnetic reconnection occurs in an asymmetric current sheet. In Run 1, the guide field $B_{y0}/B_0 = 0$, and it is antiparallel reconnection. In Runs 2 and 3, the guide field is $B_{y0}/B_0 = 0.1$ and 1.0, respectively, which represent a weak and strong guide field. In Runs

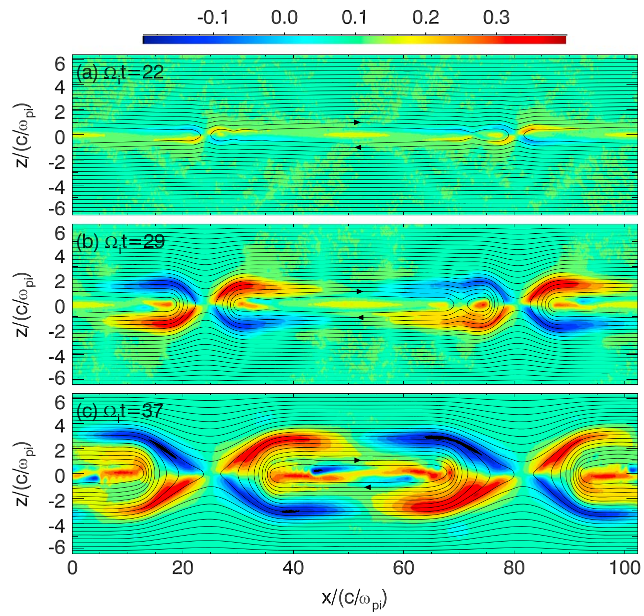

Figure 4. The time evolution of the out-of-plane magnetic field at (a) $\Omega_i t = 22$, (b) $\Omega_i t = 29$, and (c) $\Omega_i t = 37$ for Run 2. The in-plane magnetic field lines are also presented. The arrows denote the direction of the local magnetic field.

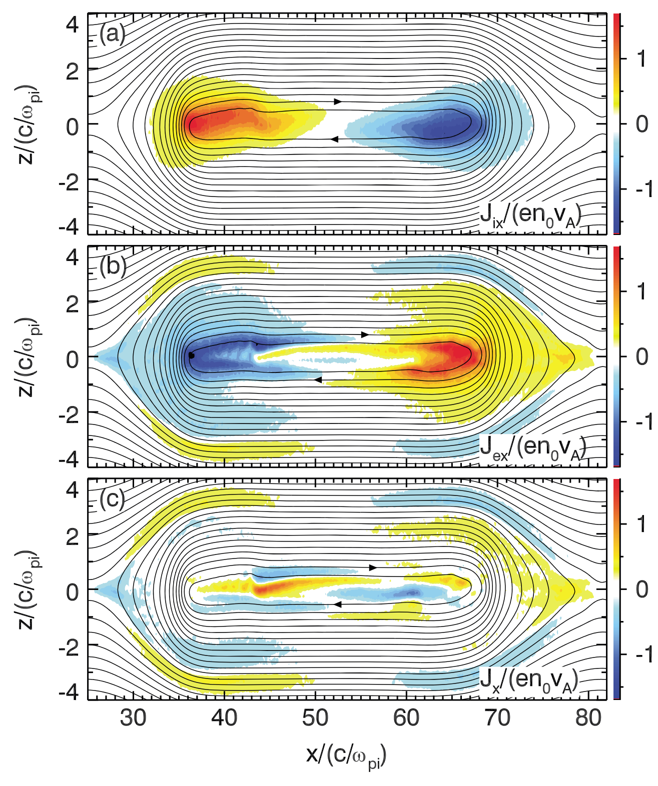

Figure 5. The (a) ion, (b) electron, and (c) total currents in the x direction at $\Omega_i t = 37$ for Run 2. The in-plane magnetic field lines are also presented. The arrows denote the direction of the local magnetic field.

4 and 5, the guide field is $B_{y0}/B_0 = 0$ and 1.0, respectively. The parameters for Runs 1–5 are summarized in Table 1.

Figure 1 shows the time evolution of the out-of-plane magnetic field B_y in Run 1. For reference, the magnetic field lines are also plotted in the figure. In this case, there is no initial guide field. With the development of the reconnection, the out-of-plane magnetic field around the X lines exhibits a characteristic quadrupole structure, whose generation mechanism has been thoroughly investigated by numerous authors [*Shay et al.*, 2001; *Pritchett*, 2001; *Nagai et al.*, 2003; *Fu et al.*, 2006; *Lu et al.*, 2010a]. Simultaneously, magnetic islands are formed between the X lines. The width of the magnetic islands increases until it saturates at about $\Omega_i t = 38$ with the width about 7.0 c/ω_{pi}. We can also find a produced secondary island around $x \sim 24$ c/ω_{pi} at $\Omega_i t = 39$. A secondary island is generated in an extended current sheet in the vicinity of an X line. In this paper, we only concern a primary island, which is formed simultaneously with the appearance of X lines during magnetic reconnection. Now let us focus on the evolution of the out-of-plane magnetic field B_y in the magnetic island between $x \sim 24$ $c/\omega_{\rm pi}$ and $x \sim 82$ $c/\omega_{\rm pi}$. At $\Omega_i t \sim 29$, a wave structure appears at the two ends of the island, which is considered to be generated due to the Weibel instability excited by the electron temperature anisotropy in the magnetic island [*Lu et al.*, 2010b]. At $\Omega_i t \sim 39$, the out-of-plane magnetic field in the center of the magnetic island also exhibits a quadrupole structure. Such a structure can last about 10 Ω_i^{-1} and then disappears.

The generation mechanism of such a quadrupole structure in the center of the island can be understood by investigating the current system in the island. Figure 2 plots the (a) ion current, (b) electron current, and (c) total current in the x direction at $\Omega_i t = 39$ for Run 1. The plasmas are accelerated by the reconnection electric field in the vicinity of the X line and then flow out along the x direction, which makes the magnetic field pile up at the two ends of the

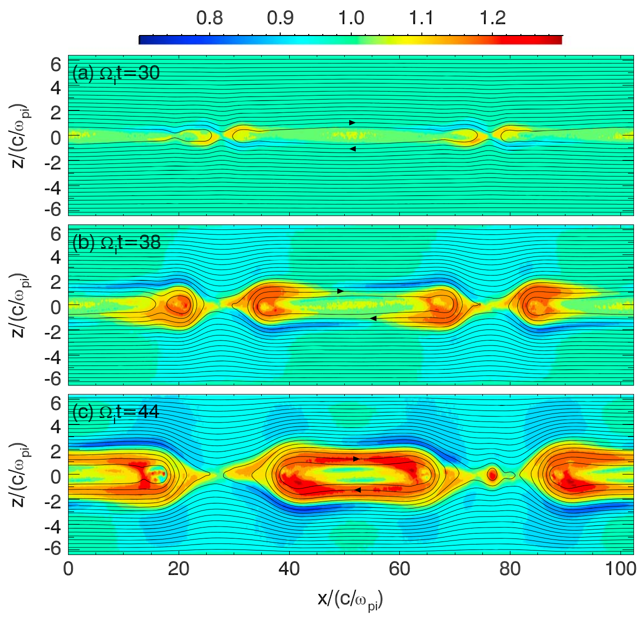

Figure 6. Similar to Figure 1 showing the snapshots of the out-of-plane magnetic field at (a) $\Omega_i t = 30$, (b) $\Omega_i t = 38$, and (c) $\Omega_i t = 44$ for Run 3. The in-plane magnetic field lines are also presented. The arrows denote the direction of the local magnetic field.

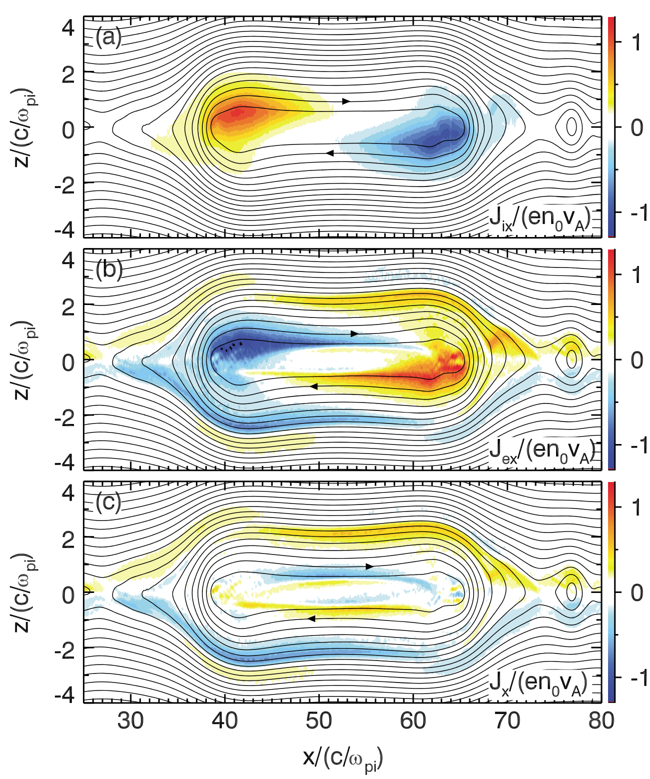

Figure 7. The (a) ion, (b) electron, and (c) total currents in the x direction at $\Omega_i t = 44$ for Run 3. The in-plane magnetic field lines are also presented. The arrows denote the direction of the local magnetic field.

island. At the same time, the island is contracted, and the electric field E_y is generated at the two ends of the island. The trapped ions and electrons in the contracted island are accelerated by the electric field at two ends of the island, and then move toward the center of the island. Such a mechanism of the electron acceleration in a magnetic island has already been studied by *Fu et al*. [2006] and *Drake et al*. [2006a]. Moreover, the behaviors of the reflected ions and electrons are different because of their different mass. The accelerated electrons are magnetized and move along the magnetic field lines, and the resulting current points toward the ends of the island. The accelerated ions are unmagnetized and move almost along the x direction toward the center of the island. Therefore, the total current system has a tripolar structure along the z direction inside the island. This can be demonstrated more clearly in Figure 3, which depicts the out-of-plane magnetic field B_y, the ion, electron, and total current in the x direction along the line $x = 45\ c/\omega_{pi}$ at $\Omega_i t = 39$. Such a current system inside the island results in the quadrupole structure of the out-of-plane magnetic field in the center of the island. When the island cannot be contracted anymore, the ions and electrons in the island cannot be accelerated. Then, both the current and the quadrupole structure of the out-of-plane magnetic field vanish in the island.

Figure 4 shows the time evolution of the out-of-plane magnetic field in Run 2. For reference, the magnetic field lines are also plotted in the figure. In this case, there is a weak initial guide field. Similar to Run 1, magnetic islands are formed between the X lines, and there is no fluctuation of the out-of-plane magnetic field, as shown in Run 1. When these magnetic islands are fully developed (at $\Omega_i t = 37$), we can also observe a quadrupole structure of the out-of-plane magnetic field in the center of these magnetic islands, although the symmetry of the quadrupole structure is now distorted. Such a structure can last about 10 Ω_i^{-1} and then disappears. Similarly,

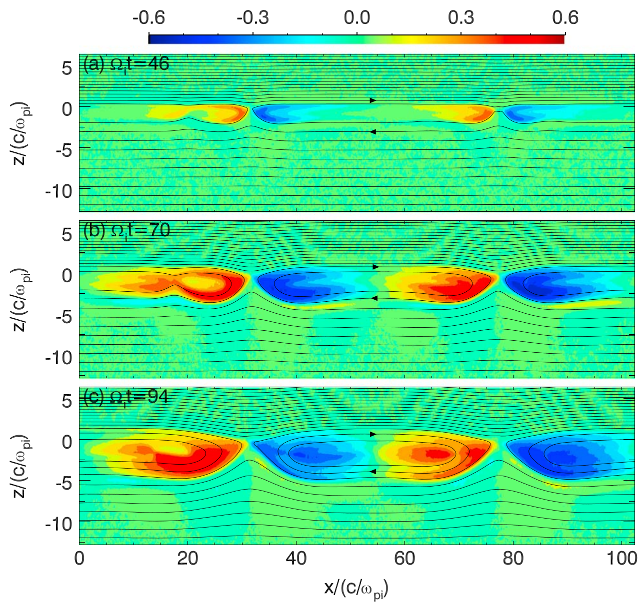

Figure 8. The time evolution of the out-of-plane magnetic field at (a) $\Omega_i t = 46$, (b) $\Omega_i t = 70$, and (c) $\Omega_i t = 94$ for Run 4. The in-plane magnetic field lines are also presented. The arrows denote the direction of the local magnetic field.

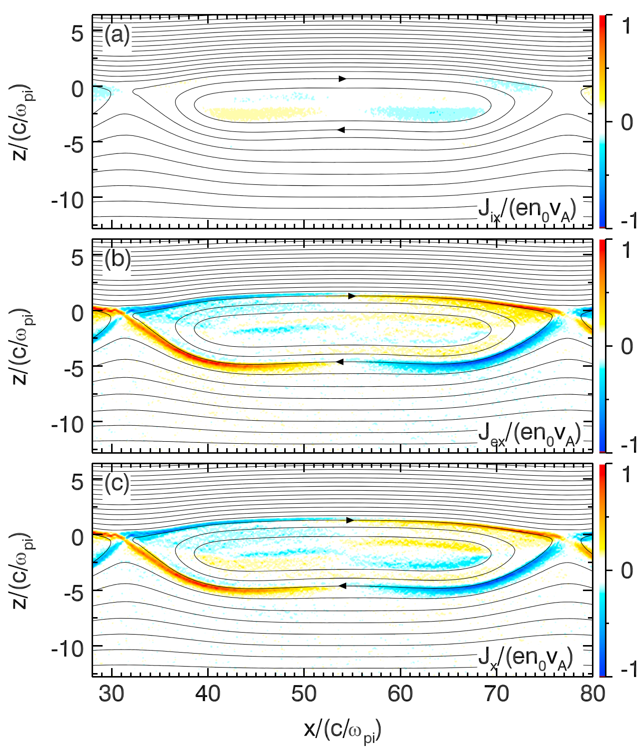

Figure 9. The (a) ion, (b) electron, and (c) total currents in the x direction at $\Omega_i t = 94$ for Run 4. The in-plane magnetic field lines are also presented. The arrows denote the direction of the local magnetic field.

the symmetry of the current system inside the magnetic islands is also distorted when a weak guide field is considered. Figure 5 plots the (a) ion current, (b) electron current, and (c) total current in the x direction at $\Omega_i t = 37$ for Run 2. Here, we only show the current system in the island between $x \sim 25c/\omega_{pi}$ and $x \sim 82c/\omega_{pi}$. When the ions and electrons move toward the center of the island after they are accelerated at the two ends of the island, they will deviate from the x direction due to the existence of the guide field. Therefore, compared with Run 1, both the current system and the quadrupole structure of the out-of-plane magnetic field inside the island are distorted.

With the increase of the initial guide field, the current system inside the magnetic island is more and more distorted. When the initial guide field is sufficiently strong, for example in Run 3 with a guide field $B_{y0} = B_0$, the total current almost forms a ring along the magnetic field lines inside the magnetic island. This can be demonstrated in Figures 6 and 7. Figure 6 plots the time evolution of the out-of-plane magnetic field at $\Omega_i t = 44$ for Run 3, while Figure 7 shows the (a) ion current, (b) electron current, and (c) total current in the x direction at $\Omega_i t = 44$ for Run 3. Here, we only show the current system in the island between $x \sim 37c/\omega_{pi}$ and $x \sim 73c/\omega_{pi}$. Both the ions and electrons are accelerated at the ends of the magnetic island; however, the electrons can be accelerated more efficiently due to their smaller mass. Thus, the total current inside the magnetic island has a ring structure. At the outer edge of the magnetic island, there is another ring of the current which is carried by the energetic electrons accelerated in the vicinity of X lines. Such a dual-ring current system results in the enhancement of the out-of-plane magnetic field inside an island with a dip in the center of the island.

We also investigate the structures of magnetic islands formed during multiple X lines in an asymmetric reconnection, where two inflow regions have different

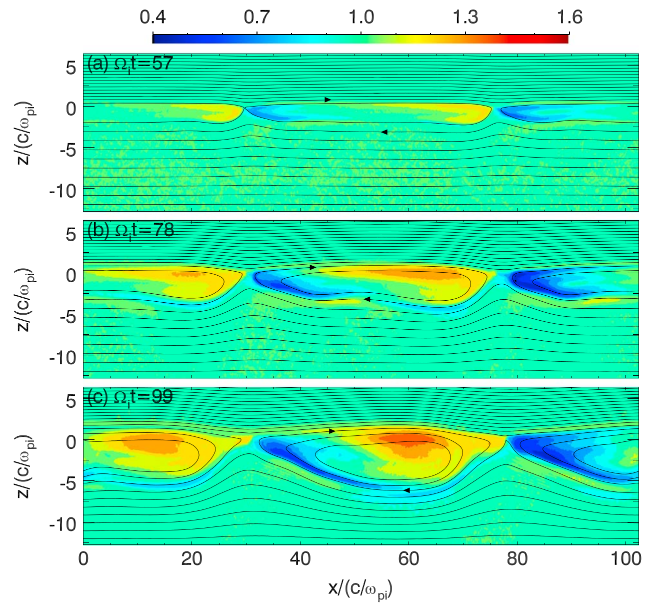

Figure 10. The time evolution of the out-of-plane magnetic field at (a) $\Omega_i t = 57$, (b) $\Omega_i t = 78$, and (c) $\Omega_i t = 99$ for Run 5. The in-plane magnetic field lines are also presented. The arrows denote the direction of the local magnetic field.

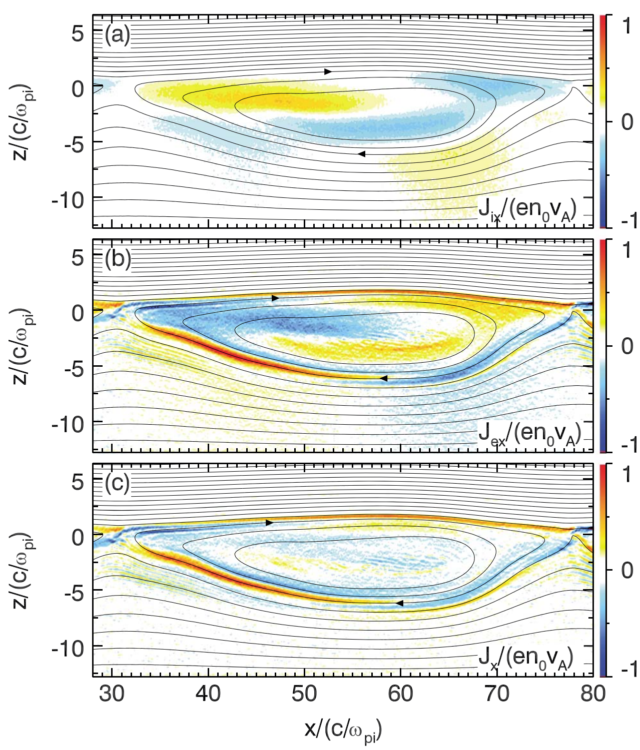

Figure 11. The (a) ion, (b) electron, and (c) total currents in the x direction at $\Omega_i t = 99$ for Run 5. The in-plane magnetic field lines are also presented. The arrows denote the direction of the local magnetic field.

plasma densities and magnetic field, like a magnetic reconnection at the magnetopause. These cases are carried out in Runs 4 and 5. Figure 8 plots the time evolution of the out-of-plane magnetic field for Run 4. For reference, the magnetic field lines are also plotted in the figure. In this case, there is no initial guide field. Magnetic islands are formed between the X lines. The rigidity of the magnetic field lines in the upper plasma sheet is stronger and more difficult to bend, so the centers of these islands move downward. When these magnetic islands are fully developed, there is a bipolar structure of the out-of-plane magnetic island along the x direction inside the island. The out-of-plane magnetic field is enhanced at one end, and is attenuated at the other end of the island. Figure 9 shows the (a) ion current, (b) electron current, and (c) total current in the x direction at $\Omega_i t = 94$ for Run 4. It is easy to find that the currents near the separatrices are carried mainly by the electrons, while the currents inside the island are small and negligible. Because the direction of the in-plane magnetic field around the magnetic island is clockwise, the blue region at the left edge of the island in Figure 9b denotes a clockwise electron flow, while the red region at the right edge denotes an anticlockwise electron flow. So the electrons flow toward the X lines along the in-plane magnetic field lines near the lower separatrices, and get accelerated by E_y in the vicinity of the X lines. Then, these electrons are directed away from the X lines along the in-plane magnetic field lines near the upper separatrices to the side with lower density. The formed currents result in the bipolar structure of the out-of-plane magnetic field along the x direction in the island, where the directions of out-of-plane magnetic field are opposite at the two ends of the island.

When a sufficiently strong guide field is introduced, the symmetries of the out-of-plane magnetic field and in-plane current systems are distorted, which are demonstrated in Figures 10 and 11.

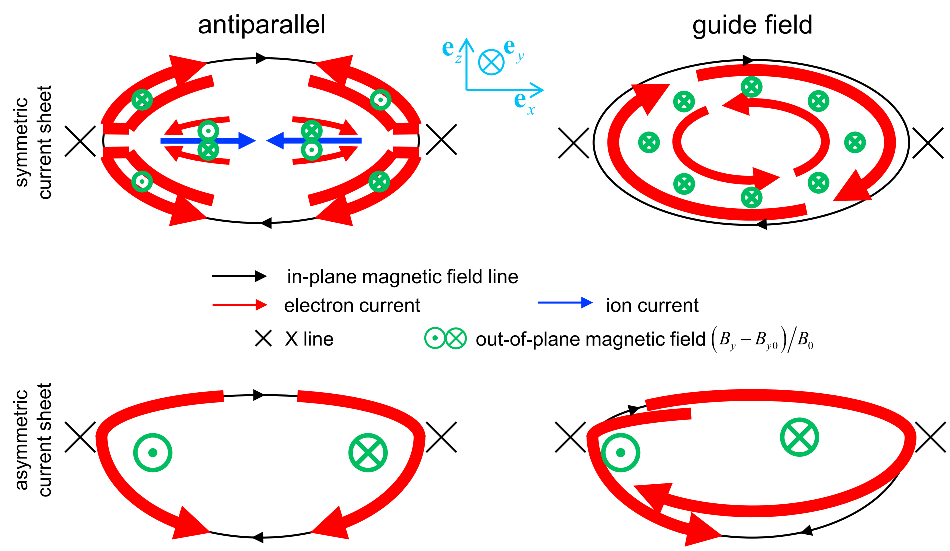

Figure 12. Sketch of the current system and magnetic structures inside a magnetic island formed during multiple X line magnetic reconnections in symmetric and asymmetric current sheets.

Figure 10 shows the time evolution of the out-of-plane magnetic field for Run 5, while Figure 11 plots the (a) ion current, (b) electron current, and (c) total current in the *x* direction at $\Omega_i t = 99$ for Run 5. We can still find an enhancement of the out-of-plane magnetic field at one end of the magnetic island, as well as attenuation at the other end. However, different from Run 4, the region where the out-of-plane magnetic field gets enhanced moves to the upper part of the island, while the region with the attenuation of the out-of-plane magnetic field is deviated to the lower part of the island. Such a structure of the out-of-plane magnetic field is caused due to the asymmetric electron currents in the vicinity of the separatrices, as shown in Figure 10.

4. Conclusions and Discussion

In this paper, 2-D PIC simulations are carried out to study the structures of magnetic islands formed during collisionless magnetic reconnection in symmetric and asymmetric current sheets, and the effects of the guide field are considered. In a symmetric plasma sheet without an initial guide field, a quadrupole structure of the out-of-plane magnetic field appears inside a magnetic island, which is caused by the ion and electron beams reflected and accelerated at the two ends of the island. When a weak guide field is introduced, the quadrupole structure of the out-of-plane magnetic field inside a magnetic island is distorted, which is not just a symmetric fluctuation superimposed upon the guide field. The structures inside the island are deviated from the line $z = 0$ due to $\mathbf{j}_{i,e} \times \mathbf{B}_{\mathrm{guide}}$ forces acted on the particles. When the guide field becomes sufficiently strong, a dual-ring current system, which is attributed to the electron dynamics in the magnetic island, is formed in a magnetic island, and it leads to an enhancement of the out-of-plane magnetic field inside the island with a dip in the center. During antiparallel reconnection in an asymmetric current sheet, electrons flow toward the X lines along the lower separatrices, and are then directed away from the X lines along the upper separatrices. The formed current results in the enhancement of the out-of-plane magnetic field at one end of the magnetic island, and the attenuation at the other end. With the increase of the guide field, the structures of both the current system and the out-of-plane magnetic field are distorted. Figure 12 summarizes the above in-plane current system and out-of-plane magnetic structures inside a magnetic island generated during multiple X line magnetic reconnections in symmetric and asymmetric current sheets.

The factors, such as the strength of the guide field and the asymmetry of the current sheet, can lead to various magnetic structures of a magnetic island formed during magnetic reconnection. Therefore, it is not strange that recent observations on the structures of magnetic islands are quite different. Our work only offers rough results on the structures of magnetic island. In reality, the structures of a magnetic island may be more complicated than that obtained in our simulations.

Acknowledgments
This research was supported by the National Science Foundation of China, grants 41204103, 11220101002, 11235009, 41274144, and 41121003; 973 Program (2013CBA01503 and 2012CB825602); Ph.D. Programs Foundation of Ministry of Education of China (20123402120010); and the open research fund from SOA Key Laboratory for Polar Science (KP201205).

Philippa Browning thanks Meng Zhou and an anonymous reviewer for their assistance in evaluating this paper.

References

Angelopoulos, V., et al. (2008), Response to comment on "Tail reconnection triggering substorm onset," *Science*, 324, 1391-c.

Baker, D. N., T. I. Pulkkinen, V. Angelopoulos, W. Baumjohann, and R. L. McPherron (1996), Neutral line model of substorms: Past results and present view, *J. Geophys. Res.*, *101*, 12,975–13,010.

Birdsall, C. K., and A. B. Langdon (1985), *Plasma Physics via Computer Simulation*, pp. 351–359, McGraw-Hill, New York.

Birn, J., et al. (2001), Geospace Environmental Modeling (GEM) magnetic reconnection challenge, *J. Geophys. Res.*, *106*, 3715–3719, doi:10.1029/1999JA900449.

Biskamp, D. (2000), *Magnetic Reconnection in Plasmas*, p. 3, Cambridge Univ. Press, Cambridge, U. K.

Borg, A. L., M. G. G. T. Taylor, and J. P. Eastwood (2012), Observations of magnetic flux ropes during magnetic reconnection in the Earth's magnetotail, *Ann. Geophys.*, *30*, 761–773, doi:10.5194/angeo-30-761-2012.

Chen, L. J., et al. (2008), Observation of energetic electrons within magnetic islands, *Nat. Phys.*, *4*, 19–23, doi:10.1038/nphys777.

Daughton, W., V. Roytershteyn, H. Karimabadi, L. Yin, B. J. Albright, B. Bergen, and K. J. Bowers (2011), Role of electron physics in the development of turbulent magnetic reconnection in collisionless plasmas, *Nat. Phys.*, *7*, 539–542, doi:10.1038/nphys1965.

Deng, X. H., H. Matsumoto, H. Kojima, T. Mukai, R. R. Anderson, W. Baumjohann, and R. Nakamura (2004), Geotail encounter with reconnection diffusion region in the Earth's magnetotail: Evidence of multiple X lines collisionless reconnection?, *J. Geophys. Res.*, *109*, A05206, doi:10.1029/2003JA010031.

Dong, Q. L., et al. (2012), Plasmoid ejection and secondary current sheet generation from magnetic reconnection in laser-plasma interaction, *Phys. Rev. Lett.*, *108*, 215001.

Drake, J. F., M. Swisdak, H. Che, and M. A. Shay (2006a), Electron acceleration from contracting magnetic islands during reconnection, *Nature*, *443*, 553–556, doi:10.1038/nature05116.

Drake, J. F., M. Swisdak, K. M. Schoeffler, B. N. Rogers, and S. Kobayashi (2006b), Formation of secondary islands during magnetic reconnection, *Geophys. Res. Lett.*, *33*, L13105, doi:10.1029/2006GL025957.

Fu, X. R., Q. M. Lu, and S. Wang (2006), The process of electron acceleration during collisionless magnetic reconnection, *Phys. Plasmas*, *13*, 012309.

Giovanelli, R. G. (1946), A theory of chromospheric flares, *Nature*, *158*, 81, doi:10.1038/158081a0.

Harris, E. G. (1962), On a plasma sheath separating regions of oppositely directed magnetic field, Nuovo Cimento Soc, *Ital. Fis.*, *23*, 115–121, doi:10.1007/BF02733547.

Huang, C., Q. M. Lu, and S. Wang (2010), The mechanisms of electron acceleration in antiparallel and guide field magnetic reconnection, *Phys. Plasmas*, *17*, 072306, doi:10.1063/1.3457930.

Huang, C., Q. M. Lu, H. Zhang, M. Y. Wu, Q. L. Dong, S. Lu, and S. Wang (2012), Kinetic simulations of the structures of magnetic island in multiple X line guide field reconnection, *Phys. Plasmas*, *19*, 042111, doi:10.1063/1.4704799.

Ji, H. T., M. Yamada, S. Hsu, and R. Kulsrud (1998), Experimental test of the Sweet-Parker model of magnetic reconnection, *Phys. Rev. Lett.*, *80*, 3256–3259.

Karimabadi, H., D. Krauss-Varban, N. Omidi, and H. X. Vu (1999), Magnetic structure of the reconnection layer and core field generation in plasmoids, *J. Geophys. Res.*, *104*, 12,313–12,326, doi:10.1029/1999JA900089.

Karimabadi, H., J. D. Huba, D. Krauss-Varban, and N. Omidi (2004), On the generation and structure of the quadrupole magnetic field in the reconnection process: Comparative simulation study, *Geophys. Res. Lett.*, *31*, L07806, doi:10.1029/2004GL019553.

Le, A., H. Karimabadi, J. Egedal, V. Royershteyn, and W. Daughton (2012), Electron energization during magnetic island coalescence, *Phys. Plasmas*, *19*, 072120, doi:10.1063/1.4739244.

Li, C. K., F. H. Seguin, J. A. Frenje, J. R. Rygg, R. D. Petrasso, R. P. J. Town, O. L. Landen, J. P. Knauer, and V. A. Smalyuk (2007), Observation of Megagauss-field topology changes due to magnetic reconnection in laser-produced plasmas, *Phys. Rev. Lett.*, *99*, 055001.

Liu, C. X., S. P. Jin, F. S. Wei, Q. M. Lu, and H. A. Yang (2009), Plasmoid-like structures in multiple X line Hall MHD reconnection, *J. Geophys. Res.*, *114*, A10208, doi:10.1029/2009JA014257.

Lu, Q. M., C. Huang, J. L. Xie, R. S. Wang, M. Y. Wu, A. Vaivads, and S. Wang (2010a), Features of separatrix regions in magnetic reconnection: Comparison of 2-D particle-in-cell simulations and Cluster observations, *J. Geophys. Res.*, *115*, A11208, doi:10.1029/2010JA015713.

Lu, S., Q. M. Lu, X. Shao, P. H. Yoon, and S. Wang (2010b), Weibel instability and structures of magnetic island in anti-parallel collisionless magnetic reconnection, *Phys. Plasmas*, *18*, 072105, doi:10.1063/1.3605029.

Lu, S., Q. M. Lu, C. Yang, C. Huang, J. L. Xie, and S. Wang (2011), The effects of the guide field on the structures of electron density depletions in collisionless magnetic reconnection, *Chin. Sci. Bull.*, *56*, 48–52, doi:10.1007/s11434-010-4250-9.

Lui, A. T. Y., M. W. Dunlop, H. Rème, L. M. Kistler, G. Gustafsson, and Q. G. Zong (2007), Internal structure of a magnetic flux rope from Cluster observations, *Geophys. Res. Lett.*, *34*, L07102, doi:10.1029/2007GL029263.

Ma, Z. W., A. Otto, and L. C. Lee (1994), Core magnetic field enhancement in single X line, multiple X line and patchy reconnection, *J. Geophys. Res.*, *99*, 6125–6136, doi:10.1029/93JA03480.

Masuda, S., T. Kosugi, H. Hara, and Y. Ogawara (1994), A loop top hard X-ray in a compact solar-flare as evidence for magnetic reconnection, *Nature*, *371*, 495–497.

Nagai, T., I. Shinohara, M. Fujimoto, S. Machida, R. Nakamura, Y. Saito, and T. Mukai (2003), Structure of the Hall current system in the vicinity of the magnetic reconnection site, *J. Geophys. Res.*, *108*(A10), 1357, doi:10.1029/2003JA009900.

Nagai, T., M. Fujimoto, Y. Saito, S. Machida, T. Terasawa, R. Nakamura, T. Yamamoto, T. Mukai, A. Nishida, and S. Kokubun (1998), Structure and dynamics of magnetic reconnection for substorm onsets with Geotail observations, *J. Geophys. Res.*, *103*(A3), 4419–4440, doi:10.1029/97JA02190.

Øieroset, M., T. D. Phan, M. Fujimoto, R. P. Lin, and R. P. Lepping (2001), In situ detection of collisionless reconnection in the Earth's magnetotail, *Nature*, *412*, 414–417, doi:10.1038/35086520.

Oka, M., M. Fujimoto, I. Shinohara, and T. D. Phan (2010a), "Island surfing" mechanism of electron acceleration during magnetic reconnection, *J. Geophys. Res.*, *115*, A08223, doi:10.1029/2010JA015392.

Oka, M., T. D. Phan, S. Krucker, M. Fujimoto, and I. Shinohara (2010b), Electron acceleration by multi-island coalescence, *Astrophys. J.*, *714*, 915–926, doi:10.1088/0004-637x/714/1/915.

Priest, E., and T. Forbes (2000), *Magnetic Reconnection: MHD Theory and Applications*, p. 6, Cambridge Univ. Press, Cambridge, U. K.

Pritchett, P. L. (2001), Geospace Environment Modeling magnetic reconnection challenge: Simulations with a full particle electromagnetic code, *J. Geophys. Res.*, *106*(A3), 3783–3798, doi:10.1029/1999JA001006.

Pritchett, P. L. (2008), Energetic electron acceleration during multi-island coalescence, *Phys. Plasmas*, *15*, 102105, doi:10.1063/1.2996321.

Pritchett, P. L., and F. V. Coroniti (2004), Three-dimensional collisionless magnetic reconnection in the presence of a guide field, *J. Geophys. Res.*, *109*, A01220, doi:10.1029/2003JA009999.

Quest, K. B., and F. V. Coroniti (1981), Tearing at the dayside magnetopause, *J. Geophys. Res.*, *86*, 3289–3298, doi:10.1029/JA086iA05p03289.

Shay, M. A., J. F. Drake, B. N. Rogers, and R. E. Denton (2001), Alfvénic collisionless magnetic reconnection and the Hall term, *J. Geophys. Res.*, *106*, 3759–3772, doi:10.1029/1999JA001007.

Sonnerup, B. U. Ö. (1979), Magnetic field reconnection, in *Solar System Plasma Physics*, vol. 3, edited by L. J. Lanzerotti, C. F. Kennel, and E. N. Parker, p. 46, North-Holland Publishing Co., Amsterdam.

Tanaka, K. G., M. Fujimoto, S. V. Badman, and I. Shinohara (2011), Dynamic magnetic island coalescence and associated electron acceleration, *Phys. Plasmas*, *18*, 022903, doi:10.1063/1.3554660.

Terasawa, T. (1983), Hall current effect on tearing mode instability, *Geophys. Res. Lett.*, *10*, 475–478, doi:10.1029/GL010i006p00475.

Vasyliunas, V. M. (1975), Theoretical models of magnetic field line merging, *Rev. Geophys.*, *13*, 303–336, doi:10.1029/RG013i001p00303.

Wang, R. S., Q. M. Lu, A. M. Du, and S. Wang (2010), In situ observations of a secondary magnetic island in ion diffusion region and associated energetic electrons, *Phys. Rev. Lett.*, *104*, 175003, doi:10.1103/PhysRevLett.104.175003.

Zhang, Q. H., et al. (2011), Coordinated Cluster/Double Star and ground-based observations of dayside reconnection signatures on 11 February 2004, *Ann. Geophys.*, *29*, 1827–1847, doi:10.5194/angeo-29-1827-2011.